

# Natural Reweighted Wake-Sleep

Csongor Várady<sup>1</sup>, Riccardo Volpi<sup>2</sup>, Luigi Malagò<sup>2</sup>, and Nihat Ay<sup>1</sup>

<sup>1</sup>Institute for Data Science Foundations, Hamburg University of  
Technology, Hamburg, Germany

<sup>2</sup>Transylvanian Institute of Neuroscience, Cluj-Napoca, Romania

## Abstract

Helmholtz Machines (HMs) are a class of generative models composed of two Sigmoid Belief Networks (SBNs), acting as an encoder and a decoder. These models are commonly trained using a two-step optimization algorithm called Wake-Sleep (WS) and more recently by improved versions, such as the Reweighted Wake-Sleep (RWS) and Bidirectional Helmholtz Machines (BiHM). The locality of the connections in a SBN induces sparsity in the Fisher information matrix associated to the model, in the form of a finely-grained block-diagonal structure. In this paper we exploit this property to efficiently train SBNs and HMs using the natural gradient. We present a novel algorithm called Natural Reweighted Wake-Sleep (NRWS), which corresponds to a geometric adaptation of the Reweighted Wake-Sleep, where, differently from most of the previous work, the natural gradient is computed without the need of introducing any approximation of the structure of the Fisher Information Matrix. The experiments performed on standard datasets from the literature show a consistent improvement of NRWS not only with respect to its non-geometric baseline but also with respect to state-of-the-art training algorithms for HMs. The improvement is quantified both in terms of speed of convergence as well as value of the log-likelihood reached after training.

**Keywords**— Natural Gradient , Helmholtz Machine, Wake Sleep Algorithm, Information Geometry

## 1 Introduction

Deep generative models have been successfully employed in unsupervised learning to model complex and high dimensional distributions thanks to their ability to extract higher-order representations of the data and thus generalize better [1, 2]. An approach which proved to be successful and thus common to several models is based on the use of two separate networks: the recognition network, i.e., the encoder, which provides a compressed latent representation for the input data, and the generative network, i.e., the decoder, able to reconstruct the

observation in output. AutoEncoders (AEs) [3] are a classical example of this paradigm, where both the encoder and the decoder are commonly implemented as deterministic feed-forward networks. Variational AutoEncoders (VAEs) [4, 5] introduce an approximate posterior distribution over the latent variables which are then sampled, thus resulting in stochastic networks. In addition, Helmholtz Machines (HMs) [6] consist of a recognition and a generative network both modelled as Sigmoid Belief Network (SBNs) [7], characterized by discrete hidden variables, differently from standard VAEs which commonly adopt continuous Gaussian variables only in the bottleneck layer.

The training of stochastic networks is a challenging task in deep learning [8]. This extends to generative models based on stochastic networks, which are commonly trained by the maximization of the likelihood or equivalently by the minimization of a divergence function between the unknown distribution of the data and the one of the generative model. The challenges for the optimization task are due to the presence of terms which are computationally expensive to be estimated, such as the partition function. A solution to this problem consists in the introduction of a family of tractable approximate posterior distributions, parameterized by the encoder network. In the presence of continuous hidden variables, for which the stochastic back-propagation of the gradient is possible, as in VAEs, the two networks can be trained simultaneously, through the definition of a unique loss function which corresponds to a lower-bound for the likelihood, i.e., the ELBO [4, 5]. In presence of discrete hidden variables, as for HMs, this approach cannot be directly employed, and thus standard training procedures relies on the well-known Wake-Sleep [9] algorithm, in which two optimization steps for the parameters of the recognition and generative networks are alternated. The Wake-Sleep algorithm, as well as more recent advances [10, 11, 12, 13], relies on the conditional independence assumption between the hidden variables of each layer, which allows a factorization of the loss function associated to directed graphical models [14]. This leads to a computationally efficient formula for the weights update which does not require the gradients to be back-propagated through the full network. An alternative to Wake-Sleep for HMs is given by the REINFORCE algorithm [15], which is popular in the Reinforcement Learning literature. However, differently from Wake-Sleep, with REINFORCE the variance of the gradient grows linearly with the number of the parameters of the network, an issue addressed in several modern variants [16, 17, 18, 19].

Besides the choice of the specific loss function to be optimized, depending on the nature of the generative model, in the literature several approaches to speed-up the convergence during training have been proposed, through the definition of different optimization algorithms. One line of research, initiated by Amari and co-workers [20, 21], takes advantage of a geometric framework based on notions of Information Geometry [22], which leads to the definition of the natural gradient. Whenever the loss function is defined over a statistical manifold of distributions, whose geometry is given by the Fisher-Rao Information metric, the natural gradient of the function to be optimized corresponds to the Riemannian gradient of the function itself computed with respect to the metric of the manifold. In general the computation of the natural gradient requires the inversion of the

Fisher Information Matrix (FIM), and for this reason often it cannot be directly applied for the training of large neural network due to its computation cost. Several approaches have been proposed in the literature [23, 24, 25, 26, 27] which are all based on more or less sophisticated approximations of the structure of the FIM. By introducing different forms of independence assumptions between random variables from the network, certain blocks of the FIM are set to zero or alternatively they admit specific representations (such as low-rank updates of a diagonal matrix or Kronecker products of matrices) which allow its efficient inversion. Instead, a different view is provided by Sun and Nielsen [28], which propose to compute a local version of the Fisher-Rao metric, that they call Relative Fisher Information Metric, used to analyze the local learning dynamics in a large system.

The use of the natural gradient for the training of generative models has been exploited in particular in the works of Lin et. al. Zhang et. al. [29, 30]. In this paper we follow a different approach for the computation of the natural gradient for the training of a HM which does not require an approximation of the FIM before its empirical evaluation.

Motivated by preliminary results from [31] for the computation of the FIM for a SBN, we observe that the matrix associated with the joint statistical model represented by a HM takes a block-diagonal structure, where the block sizes depend linearly on the size of each hidden layer. This result, which can be seen as a direct consequence of the topology of the directed graphical model associated to the SBN, does not require the introduction of any additional independence assumption between random variables in the FIM, before its empirical evaluation. Notice that the level of sparsity for the FIM in SBNs is superior to that associated to the standard assumption of independence between layers, where the width of the blocks is given by the product of the sizes of adjacent hidden layers. Indeed for SBN we have a finely-grained block-diagonal structure for the FIM, with block widths given by the sizes of the hidden layers, which allows a more computationally efficient inversion of the matrix. Based on these observations we propose an efficient geometric adaptation of the Reweighted Wake-Sleep algorithm for the training of HMs, where the gradient is replaced by the corresponding natural gradient. The intrinsic sparsity of the FIM, which is a direct consequence of the topology of the network, limits the impact on the cost per iteration. This has the advantage to allow for an exact computation of the natural gradient for a given batch, not requiring further assumptions in terms of structure of the FIM, thus taking advantage of the speed-up in convergence during training, while limiting the computational overhead. Our main contributions are the following:

1. The design of a novel algorithm (NRWS) based on Natural Gradient (NG) for the training of HMs which exploits a finely-grained block-diagonal structure for the FIM. Such structure for the FIM: a) has never been exploited before in the training of HMs, not even for deterministic networks, as a matter of fact [31] does not refer to any application in training; b) differently from other models it is exact, i.e., for HM the sparsity struc-

ture is not an approximation/assumption but it derives from conditional independence among variables set by the network topology; c) is made of smaller-sized blocks (thus it is more efficient to be computed) than the standard block-diagonal structure used in previous works. [28, 30]

2. Our results on 3 datasets show that we are able not only to converge to a better value for the loss both in training and test compared to RWS and BiHM (SOA in the literature for HM), but also to achieve faster convergence, both in terms of epochs and wall-clock time. This is a strong result, since NG often suffers from large computation complexity which prevents its use in practice.

The paper is organized as follows. First in Sections 2 and 3 we briefly present the Helmholtz Machine, the Wake-Sleep and the Reweighted Wake-Sleep algorithms. In Sections 4 and 5 we introduce the natural gradient and the FIM, describing its block structure in the case of a HM. In Section 6 we define the Natural Reweighted Wake-Sleep Algorithm. Finally in Sections 9 and 10 we discuss our results and draw the conclusions.

## 2 Sigmoid Belief Networks and Helmholtz Machines

Sigmoid Belief Networks (SBNs) are a class of models corresponding to a sequence of stochastic layers, one on top of the other, where the first layer is the visible layer, while the others are hidden layers. The activation on each layer of the SBN are Sigmoid functions the result of which serve as the means for Bernoulli distributions. Such a network can be characterized as a joint probability distribution  $p$  where

$$p(x, h) = p(x|h) p(h) , \quad (1)$$

$x$  represents the visible layer and  $h$  the hidden ones.

The Helmholtz Machine (HM) [6] is a particular case of an SBN, which has the property that each consecutive layer is connected to each other in both directions. This enables us to not only define a generation distribution  $p$  but also a recognition distribution  $q$  parameterized by  $\phi$ . The HM is illustrated in Figure 1. For  $L$  number of layers the distributions  $p$  and  $q$  factorize as follows:

$$p_{\theta}(x, h) = p(x|h_1) p(h_1|h_2) \cdots p(h_{L-1}|h_L) p(h_L) , \quad (2)$$

$$q_{\phi}(h|x) = q(h_L|h_{L-1}) \cdots q(h_2|h_1) q(h_1|x) . \quad (3)$$

Usually as we go higher in the layers, they become narrower, with the last layer  $L$  being the narrowest “bottleneck” layer. The goal of such HMs is to learn the distribution of some data distribution  $p_{\mathcal{D}}(x)$  from a dataset  $\mathcal{D}$ . Methods for

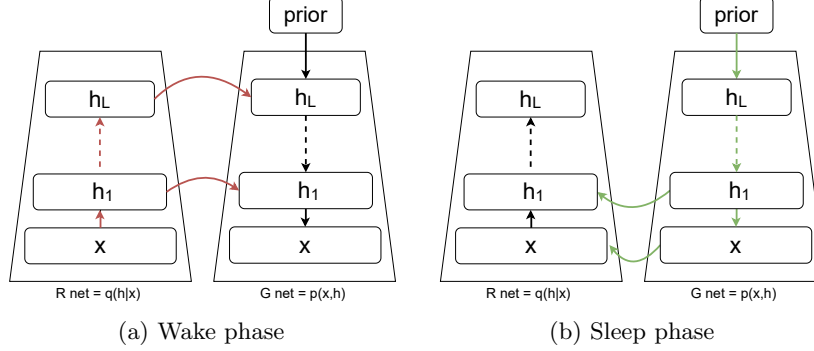


Figure 1: The structure of a Helmholtz Machine with  $L$  layers and a prior distribution. The colored arrows indicate the propagation of the samples during the Wake 1a and Sleep 1b phases. In the Wake phase the sampling is done in  $p_{\mathcal{D}}(x)$  and propagates through the recognition network  $q(h|x)$ . In the Sleep phase we sample a “dream” from the prior  $p(h_L)$  and propagate it through the generative network  $p(x, h)$ .

learning such distributions are usually minimizing the difference between the generative distribution  $p(x)$  and  $p_{\mathcal{D}}(x)$ , formalized by

$$\arg \min_{\theta} D_{KL}[p_{\mathcal{D}}(x)||p(x;\theta)] , \quad (4)$$

where  $\theta$  represent the parameters of the network and  $D_{KL}$  is the Kullback–Leibler divergence. If we expand the definition of the KL-divergence, we see that minimizing the divergence is equivalent to minimizing the negative log-likelihood of  $p(x)$  which can also be viewed as the Helmholtz Free Energy

$$\begin{aligned} \arg \min_{\theta} D_{KL}[p_{\mathcal{D}}(x)||p(x;\theta)] &= \arg \min_{\theta} \int p_{\mathcal{D}}(x) \ln \frac{p_{\mathcal{D}}(x)}{p(x;\theta)} dx \\ &= \arg \min_{\theta} \underbrace{\int p_{\mathcal{D}}(x) \ln p_{\mathcal{D}}(x) dx}_{\text{independent of } \theta} - \int p_{\mathcal{D}}(x) \ln p(x;\theta) dx \\ &= \arg \max_{\theta} \mathbb{E}_{p_{\mathcal{D}}(x)} [\ln p(x;\theta)] . \end{aligned} \quad (5)$$

Traditionally the HM is trained by Wake-Sleep algorithm [9] (WS). The WS is a two phase alternating training algorithm, where the Wake phase samples from the real distribution  $p_{\mathcal{D}}$  and learns the parameters of  $p$  by optimizing the variational free energy

$$\arg \min_{\theta} \mathcal{L}_p(x) = \arg \max_{\theta} \mathbb{E}_{p_{\mathcal{D}}(x)} [\ln p(x;\theta)] - D_{KL}[q(h|x;\phi)||p(h|x;\theta)] . \quad (6)$$

The Sleep phase optimizes parameters of  $q$  based on samples from a prior distribution (called a dream) and optimizes an augmented version of the variational free energy, where the arguments of the KL divergence are switched,

$$\arg \min_{\phi} \mathcal{L}_q(x) = \arg \max_{\phi} \underbrace{\mathbb{E}_{p_{\mathcal{D}}(x)} [\ln p(x; \theta)]}_{\text{independent of } \phi} - \underbrace{D_{KL}[p(h|x; \theta) || q(h|x; \phi)]}_{\text{args switched from (6)}} . \quad (7)$$

### 3 The Reweighted Wake-Sleep Algorithm

Following a reinterpretation due to [10], the training of Helmholtz Machines can be recast in terms of a variational objective [32, 4]. This is analogous to the learning in a Variational Autoencoder [4] which requires maximizing a lower bound of the likelihood. The derivative of the log-likelihood of a single sample  $x$  can be approximated with a Monte Carlo sampling [10, 33] by running it through the the network  $S$  times

$$\begin{aligned} \frac{\partial \mathcal{L}_p(x \sim p_{\mathcal{D}}(x))}{\partial \theta} &= \frac{1}{p(x)} \mathbb{E}_{h \sim q(h|x)} \left[ \frac{p(x, h)}{q(h|x)} \frac{\partial \ln p(x, h)}{\partial \theta} \right] \\ &\simeq \sum_{k=1}^S \tilde{\omega}_k \frac{\partial \ln p(x, h^{(k)})}{\partial \theta} \text{ with } h^{(k)} \sim q(h|x) . \end{aligned} \quad (8)$$

This is called **p-wake update**. The last step is involving the Monte Carlo approximation of the expectation value with importance weights

$$\tilde{\omega}_k = \frac{\omega_k}{\sum_{k'} \omega_{k'}} , \text{ with } \omega_k = \frac{p(x, h^{(k)})}{q(h^{(k)}|x)} . \quad (9)$$

The quantity being optimized in Equation (8) is also referred to as Reconstruction Likelihood (RL) and the optimization is performed in function of the parameters of the generation network  $\theta$ . The approximate posterior depends also from another set of parameters  $\phi$ .  $q$  can be optimized by minimizing the variance of the Monte Carlo estimation in Eq. (8), or equivalently by minimizing the KL divergence with the generative posterior [10, 33]. This can be averaged sampling  $x$  from the true data distribution  $p_{\mathcal{D}}(x)$  (**q-wake update**) with  $h^{(k)} \sim q(h|x)$

$$\frac{\partial \mathcal{L}_q^w(x \sim p_{\mathcal{D}}(x))}{\partial \phi} \simeq \sum_{k=1}^S \tilde{\omega}_k \frac{\partial \ln q(h^{(k)}|x)}{\partial \phi} \text{ with } h^{(k)} \sim q(h|x); \quad (10)$$

or it can be averaged over samples  $x, h$  from the generative model  $p(x, h)$  (**q-sleep update**) with  $x^{(k)}, h^{(k)} \sim p(x, h)$

$$\frac{\partial \mathcal{L}_q^s((x, h) \sim p(x, h))}{\partial \phi} \simeq \sum_{k=1}^S \frac{\partial \ln q(h^{(k)}|x^{(k)})}{\partial \phi} . \quad (11)$$

The algorithm just described is called Reweighted Wake-Sleep (RWS) [10, 33]. The q-sleep update it is commonly known as sleep phase in the classical Wake-Sleep (WS) [6, 9] algorithm, which only uses the p-wake update and the q-sleep update, both with  $S = 1$  sample.

## 4 Natural Gradient

Information Geometry [34, 22, 35, 36] studies the geometry of statistical models using the language of Riemannian geometry, representing a set of probability distributions  $\mathcal{M} = \{p = p_\theta : \theta \in \Theta\}$  as a manifold. The parametrization  $\theta$  for  $p$  identifies a set of coordinates, i.e., a chart, over the manifold. Similarly, it is possible to define the tangent space  $T_p\mathcal{M}$  in each point as the set of the velocity vectors along all the curves which pass through in  $p$ . In Information Geometry, statistical manifolds are commonly endowed with a Riemannian Fisher-Rao metric over the tangent bundle defined by the expected value in  $p$  of the product of two tangent vectors, represented by centered random variables. Given a basis for the tangent space, derived from the choice of the parametrization, the inner product associated to the Fisher-Rao metric is represented through a quadratic form expressed through the Fisher information matrix  $\mathcal{F}$ . Given a real-valued function  $\mathcal{L}$  defined over the statistical manifold  $\mathcal{M}$ , the direction of steepest ascent is represented by the Riemannian gradient of  $\mathcal{L}$  whose evaluation depends on the metric. Let  $\nabla\mathcal{L}$  denote the vector of partial derivatives  $\frac{\partial}{\partial\theta}\mathcal{L}(p)$  in the chosen chart. These represent the coordinates of a covector,  $\frac{\partial}{\partial\theta}\mathcal{L}(p) \in T_p^*\mathcal{M}$ . The natural gradient is the vector in  $T_p\mathcal{M}$  associated to  $\nabla\mathcal{L}$  through the canonical isomorphism between tangent and cotangent space induced by the metric [20, 21], i.e.,

$$\tilde{\nabla}\mathcal{L}(\theta) = \mathcal{F}(\theta)^{-1}\nabla\mathcal{L}(\theta) , \quad (12)$$

with

$$\mathcal{F}(\theta) = \mathbb{E}_p \left[ \frac{\partial}{\partial\theta} \log p(\theta) \left( \frac{\partial}{\partial\theta} \log p(\theta) \right)^T \right] = -\mathbb{E}_p \left[ \frac{\partial^2}{\partial\theta\partial\theta} \log p(\theta) \right] . \quad (13)$$

The natural gradient descent update then takes the form of

$$\theta_{t+1} = \theta_t - \eta \tilde{\nabla}\mathcal{L}(\theta) , \quad (14)$$

where  $\theta_t$  are the weights at step  $t$  and  $\eta$  is the learning rate.

## 5 Fisher Information Matrix for Helmholtz Machines

The computation of the Fisher information matrix, needed in order to compute the natural gradient of a given loss function, strongly depends on the nature

of the statistical model with respect to which the loss is defined. We refer the reader to [37] for the computation in the case of feed-forward networks for classification and regression problems. In this section we show how the FIM in Eq. (13) can be rewritten in the case of Sigmoid Belief Networks (SBN), which constitute the building blocks for Helmholtz Machines. The FIM for directed acyclic graphical models takes a simplified block-diagonal form thanks to the locality of connection matrix, given by the conditional independence the random variables. This result has been exploited recently in the training of stochastic feed-forward neural networks, see for instance Thm. 3 from [28], leading to a block-diagonal FIM, with one block per layer, a structure also assumed by [24, 25]. However, by a direct generalization to deep stochastic networks of a result from [31] for a two-layers networks, it is easy to show that SBNs admit an FIM with a finer-grained block structure, consisting of one block per neuron. The following proposition formalizes this result, while Fig. 2 provides a graphical representation.

**Proposition 1.** *Let  $\mathcal{G}$  be a directed acyclic graphical model, whose variables are grouped in layers such that each node from the  $i$ -th layer has parent nodes from the  $(i - 1)$ -th layer only. The FIM associated to the joint probability distribution  $p$  that factorizes as the product of conditional distributions according to  $\mathcal{G}$  has a block-diagonal structure, with one block for each hidden unit of size equal to the number of parent nodes.*

The proof of this result is based on a generalization of Theorem 1 from [38] (see also Lemma 1 in [31]). However, we would like to point out that the works [31] and [38] do not refer to any application in training.

## 5.1 Fisher Information Matrix of a Sigmoid Belief Network

Let us consider a Helmholtz Machine with  $L$  layers  $h^{(i)}$ , the 0-th layer  $h^{(0)} = x$  is also called the visible layer. The generation network introduces a prior  $p_{\theta^{(L)}}$  on the top most layer  $L$ , leading to the factorization

$$p_{\theta}(x, h) = p_{\theta^{(L)}}(h^{(L)}) \prod_{i=L-1}^0 p_{\theta^{(i)}}(h^{(i)} | h^{(i+1)}), \quad (15)$$

and it is parameterized by  $\theta^{(i)}$  with weights  $W^{(i)}$  and biases  $b^{(i)}$  at each layer  $i$ , for  $i = 0, \dots, L$ .

For each neuron  $r$  of the layer  $i$ ,  $p(h_r^{(i)} | h^{(i+1)})$  is a Bernoulli distribution depending on the previous layer

$$\sigma(W_r^{(i)} h^{(i+1)} + b_r^{(i)})^{h_r^{(i)}} \left(1 - \sigma(W_r^{(i)} h^{(i+1)} + b_r^{(i)})\right)^{1-h_r^{(i)}} \quad (16)$$

where  $W_r^{(i)} \in \mathbb{R}^{l_{i+1}}$  is a vector of weights (row of  $W^{(i)}$ ) for the neuron  $r$  of the



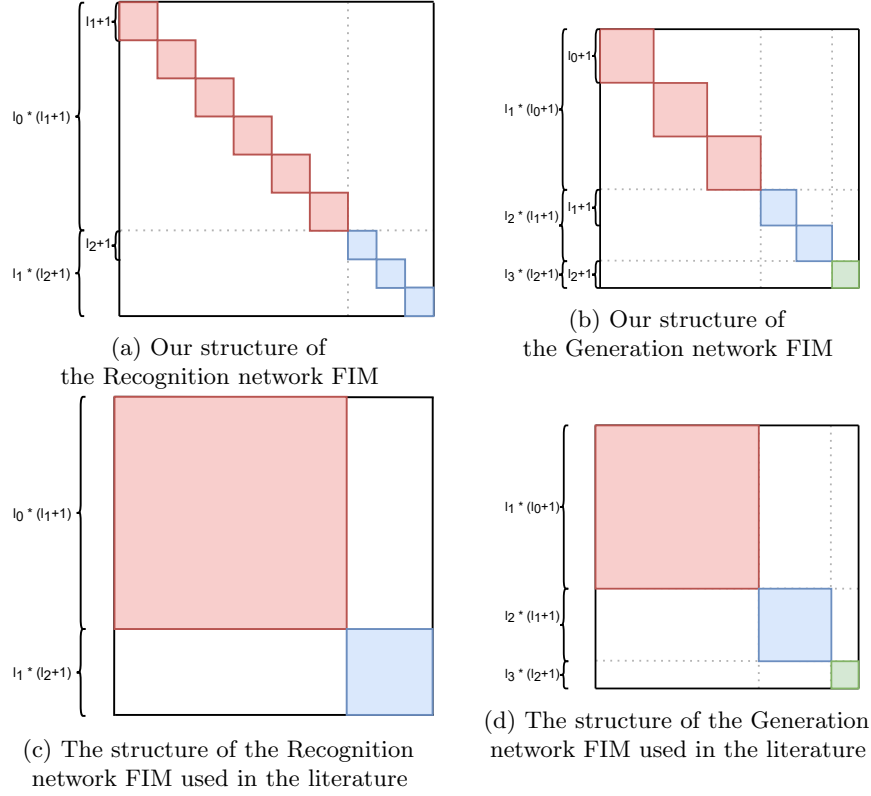


Figure 2: Graphical representation of the Fisher information matrix for a Network with 6-3-2 nodes and the prior. The gray lines identify the blocks associated to the layers of the network. The matrix admits a fine-grained block-diagonal structure with blocks of size equal to the size of the hidden layers. The blocks are ordered in both cases from the bottom layer to the top starting from the upper-left. The comparison from the literature are from the works of [24, 25, 28].

layer  $i$ , and  $b_r^{(i)}$  is a bias. Equation (16) can be also written in compact form as

$$\sigma(\widetilde{W}_r^{(i)} \widetilde{h}^{(i+1)})^{h_r^{(i)}} \left(1 - \sigma(\widetilde{W}_r^{(i)} \widetilde{h}^{(i+1)})\right)^{1-h_r^{(i)}}, \quad (17)$$

where  $h^{(i+1)}$  and  $W_r^{(i)}$  have been augmented with 1 and  $b_r^{(i)}$ , respectively. However, for brevity and readability purposes we remove the  $\sim$  and assume the same structure with the built-in bias. The second derivative of the log of Eq. (17) is

$$\frac{\partial^2}{\partial W_{rl}^{(k)} \partial W_{rm}^{(k)}} \ln p(h_r^{(i)} | h^{(i+1)}) = -\sigma' \left( W_r^{(i)} h^{(i+1)} \right) h_l^{(i+1)} h_m^{(i+1)T}, \quad (18)$$

where  $\sigma$  is the sigmoid function used in SBN, and  $\sigma'$  is its derivative.

This leads to a natural block structure, the block of the Fisher information matrix  $\mathcal{F}$  with respect to the weights  $W_r^{(i)}$  of the distribution  $p$  is

$$\mathcal{F}_{p,r}^{(i)} = -\mathbb{E}_{p(x,h)} \left[ \frac{\partial^2}{\partial W_r^{(i)} \partial W_r^{(i)}} \ln p(h_r^{(i)} | h^{(i+1)}) \right] \quad (19)$$

$$= \mathbb{E}_{p(x,h)} \left[ \sigma' \left( W_r^{(i)} h^{(i+1)} \right) h^{(i+1)} h^{(i+1)\text{T}} \right]. \quad (20)$$

In case we would use +1 and -1 instead then

$$p(h_r^{(i)} | h^{(i+1)}) = \sigma \left( h_r^{(i)} \left( W_r^{(i)} h^{(i+1)} \right) \right), \quad (21)$$

while the formula for the the FIM would be the same as in Eq. (20).

The recognition network targets to approximate the true posterior distribution by

$$q_\phi(h|x) = \prod_{i=1}^L q_{\phi(i)}(h^{(i)} | h^{(i-1)}). \quad (22)$$

parameterized by  $\phi^{(i)}$  with weights  $V^{(i)}$  at each layer  $i$ , for  $i = 0, \dots, L-1$ . By means of the generative and discriminative networks we can define two different joint distributions over the visible and hidden variables,  $p_\theta(x, h)$  and  $q_\phi(x, h) = q_\phi(h|x)p_{\mathcal{D}}(x)$ . Both distributions correspond to a statistical manifold for which we are interested in computing the Fisher-Rao metric.

Let  $i$  denote a layer, and  $j$  one of its hidden nodes, we denote with  $W_j^{(i)}$  the  $j$ -th column of the matrix  $W^{(i)}$  for the distribution  $p$  and similarly  $V_j^{(i)}$  for  $q$ . The blocks associated to the  $i$ -th-layer and  $j$ -th hidden unit, for both  $p$  and  $q$ , read

$$\mathcal{F}_{p,j}^{(i)} = \mathbb{E}_{p(x,h)} \left[ \sigma' \left( W_j^{(i)} h^{(i+1)} \right) h^{(i+1)} h^{(i+1)\text{T}} \right] \quad \text{and} \quad (23)$$

$$\mathcal{F}_{q,j}^{(i)} = \mathbb{E}_{q(x,h)} \left[ \sigma' \left( V_j^{(i)} h^{(i-1)} \right) h^{(i-1)} h^{(i-1)\text{T}} \right]. \quad (24)$$

The result is a square matrix from the outer product of the two vectors multiplied with the scalar, where the length of the side corresponds to the size of the corresponding weights  $W_j^{(i)}$  or  $V_j^{(i)}$ , that are being updated (see Fig. 2).

## 5.2 Estimation of the Fisher Information Matrix

Notice that  $h^{(i)}$  is a stochastic quantity which can be sampled from the previous layer because of the conditional independence of the layers. We can use this fact to do a Monte Carlo estimate of each block of  $\mathcal{F}$  with  $n$  samples (for the value of  $n$  see Section 6) based on the preceding layer. Thus, Eqs. (23) and (24) can be estimated as

$$F_{p,j}^{(i)} = \frac{1}{n} \sum \sigma' \left( W_j^{(i)} h^{(i+1)} \right) h^{(i+1)} h^{(i+1)\text{T}} \quad (25)$$

$$= H^{(i+1)} Q_p^{(i)} \left( H^{(i+1)} \right)^{\text{T}} \text{ with } h^{(i+1)} \sim p(h^{(i+1)} | h^{(i+2)}) \text{ and} \quad (26)$$

$$F_{q,j}^{(i)} = \frac{1}{n} \sum \sigma' \left( V_j^{(i)} h^{(i-1)} \right) h^{(i-1)} h^{(i-1)\text{T}} \quad (27)$$

$$= H^{(i-1)} Q_q^{(i)} \left( H^{(i-1)} \right)^{\text{T}} \text{ with } h^{(i-1)} \sim q(h^{(i-1)} | h^{(i-2)}) . \quad (28)$$

In the last step we introduced a matrix representation for the empirical estimation  $F$  of the  $\mathcal{F}$ , where the  $H^{(i)}$  matrices are obtained by concatenating for each sample vector  $h^{(i)}$  as a column vector, while the diagonal matrices  $Q_p^{(i)}$  and  $Q_q^{(i)}$  depends on the evaluation of the activation function. To obtain a lower variance estimation for the expected value in (23) using samples from the distribution  $q(x, h) = q(h|x)p_{\mathcal{D}}(x)$  and reweighting them by importance sampling with the same weights  $\tilde{\omega}_k$  as in (9) we get

$$F_{p,j}^{(i)} = \frac{1}{n} \sum \tilde{\omega}_k \sigma' \left( W_j^{(i)} \tilde{h}^{(i+1)} \right) \tilde{h}^{(i+1)} \tilde{h}^{(i+1)\text{T}} \quad (29)$$

$$= \tilde{H}^{(i+1)} \tilde{Q}_p^{(i)} \left( \tilde{H}^{(i+1)} \right)^{\text{T}} \text{ with } \tilde{h}^{(i+1)} \sim q(\tilde{h}^{(i+1)} | \tilde{h}^{(i)}) . \quad (30)$$

Eqs. (26)-(29) represent the blocks of the empirical Fisher information matrices, for  $W_j^{(i)}$  and for  $V_j^{(i)}$ , respectively. Notice that the empirical estimations in Eqs. (26) and (28) are not to be confused with the approximations typically introduced for the simplification of the FIM, needed to make it computationally tractable in feed-forward neural networks. This block structure is very convenient and represents the main argument for the efficiency of the algorithm.

The FIMs in Eqs. (23) and (24) only depend on the statistical models associated to the joint distributions  $p(x, h)$  and  $q(x, h)$ , and they are independent from the specific loss function  $\mathcal{L}$  or its vector of partial derivatives  $\nabla \mathcal{L}$ , as well as from the chosen training algorithm. Hence, since the model of the Helmholtz Machine remains unchanged, the same FIMs can be used for different training algorithms (WS, RWS, etc.).

It is worth mentioning that the FIM of the visible distribution  $p(x)$  could also be derived and used for training, which could be better for approximating the real distribution of the data  $p_{\mathcal{D}}(x)$  [38], however some works [39] suggest that the FIM actually profits from the expressivity of the joint distribution  $p(x, h)$ . This derivation however presents additional complications and its computational feasibility will be explored in future works.

## 6 The Natural Reweighted Wake-Sleep Algorithm

In this section we introduce the Natural Reweighted Wake-Sleep (NRWS) algorithm, a geometric adaptation of Reweighted Wake-Sleep (RWS) algorithm,

where the update of the weights is obtained through the computation of the natural gradient of the different loss functions in the wake and sleep updates.

### 6.1 Inversion of the Fisher Information Matrix

The matrices of the form  $HQH^T$  associated with the estimation of the blocks of the FIM from Eqs. (26) and (28) may be singular depending on the number of samples in the minibatch used in the estimation compared to its size. Let  $n$  be the size of the minibatch  $b$  multiplied by the number of samples  $S$  from the network (respectively  $p$  or  $q$ , depending on the FIM under consideration) and  $l_i$  the size of the layer  $i$ . Notice that during training typically  $n < l_i$ , thus to guarantee the invertibility of the estimated Fisher matrix we add to  $HQH^T$  a damping factor  $\alpha > 0$  multiplying the identity matrix as a form of Tikhonov regularization. Our regularized estimation of the FIM is then

$$\tilde{F} = \frac{\alpha \mathbb{1}_l + F}{1 + \alpha}, \quad (31)$$

so that  $\tilde{F}^{-1} \rightarrow \mathbb{1}_l$  for  $\alpha \rightarrow \infty$  and  $\tilde{F}^{-1} \rightarrow F^{-1}$  for  $\alpha \rightarrow 0$ . Notice that depending on the rank of the  $\tilde{F}$  and on its size, from a computational perspective, for the estimation of the natural gradient it is more convenient either to invert the matrix itself or to keep in memory its rank- $k$  update representation. An experimental analysis for appropriate values for  $\alpha$  can be found in Appendix A.1.

Now we can use the Sherman-Morrison formula (done similarly in [40]) to calculate the inverse of a rank- $k$  update

$$\begin{aligned} \tilde{F}^{-1} &= \left( \frac{\alpha \mathbb{1}_l + HQH^T}{1 + \alpha} \right)^{-1} \\ &= \frac{1 + \alpha}{\alpha} (\mathbb{1}_l - H(\alpha Q^{-1} + H^T H)^{-1} H^T) . \end{aligned} \quad (32)$$

By using the Sherman-Morrison formula instead of a straightforward matrix inversion in the larger layers, we reduce the theoretical complexity of the algorithm from  $\mathcal{O}(l_i^{2.32})$  to  $\mathcal{O}(l_i n + n^{2.32})$  for each block where  $l_i$  is the size of the layer ( $0 \leq i \leq L$ ) and  $n$  is the number of samples from the joint distribution. In the case where  $l_i < n$  for narrower layers at the top of the network, a direct inversion can be used.

The inversion operation for each layer  $i$  has to be done  $l_{i-1}$  times for each of the blocks in the case of  $F_p$  and  $l_{i+1}$  for  $F_q$ . A direct consequence of this is that overall complexity will be bounded by  $\mathcal{O}(l_0 (l_1 n + n^{2.32}))$  where  $l_0$  and  $l_1$  are the bottom two layers of the Helmholtz Machine, which are usually the largest.

### 6.2 K-step update

Assuming the locality of the gradient descent learning step, we make the approximation of slowly changing metric during few training steps. Under these

---

**Algorithm 1:** Natural Reweighted Wake-Sleep

---

```

1 Let  $x$  be a minibatch of samples from the dataset
2 Let  $p$  and  $q$  be the joint distributions of the generation and the
  recognition networks with weights  $W$  and  $V$ 
3 Let  $\omega_K$  be the importance weights from the RWS
4 Let  $L$  be the depth of the HM
5 #wake phase update
6 for each layer  $i$  from  $q$  ascending with  $h_0 = x$  do
7   Sample  $h^{(i+1)}$  from  $q(h^{(i+1)}|h^{(i)})$ 
8   Compute the gradients  $\nabla_p^{(i)} \mathcal{L}_p$  with respect to  $W^{(i)}$ 
9   Compute the matrices for  $(\tilde{F}_p^{(i)})^{-1}$  for the sub-blocks in  $i$  with  $h^{(i+1)}$ 
    and  $p(h^{(i)}|h^{(i+1)})$ 
10   $\tilde{\nabla}_p^{(i)} \mathcal{L}_p = \omega_K (\tilde{F}_p^{(i)})^{-1} \nabla_p^{(i)} \mathcal{L}_p$ 
11  #q-wake update
12  Calculate  $\nabla_q^{(i)} \mathcal{L}_q^w$  and  $(\tilde{F}_q^{(i)})^{-1}$  as in the Sleep phase
13   $\tilde{\nabla}_q^{(i)} \mathcal{L}_q^w = \omega_K (\tilde{F}_q^{(i)})^{-1} \nabla_q^{(i)} \mathcal{L}_q^w$ 
14  Update  $W^{(i)}$  and  $V^{(i)}$  with the  $\tilde{\nabla}_p^{(i)} \mathcal{L}_p$  and  $\tilde{\nabla}_q^{(i)} \mathcal{L}_q^w$ 
15 #sleep phase update
16 for each layer  $i$  from  $p$  descending with  $h^{(L)}$  sampled from the prior do
17   Sample  $h^{(i-1)}$  from  $p(h^{(i-1)}|h^{(i)})$ 
18   Compute the gradients  $\nabla_q^{(i)} \mathcal{L}_q^s$  with respect to  $V^{(i)}$ 
19   Compute the matrices  $(\tilde{F}_q^{(i)})^{-1}$  for the sub-blocks in  $i$  with  $h^{(i-1)}$ 
    and  $q(h^{(i)}|h^{(i-1)})$ 
20   $\tilde{\nabla}_q^{(i)} \mathcal{L}_q^s = (\tilde{F}_q^{(i)})^{-1} \nabla_q^{(i)} \mathcal{L}_q^s$ 
21  Update  $V^{(i)}$  with  $\tilde{\nabla}_q^{(i)} \mathcal{L}_q^s$ 

```

---

assumptions we can reuse the FIM for a certain amount of steps  $K$ , without recalculating it. We will call this technique, K-step update. When reusing the frozen FIM blocks the complexity of the algorithm becomes  $\mathcal{O}(l_0(l_1n + n^2))$ , however a consequence is that we are trading memory space for this speed up. Saving the FIM blocks means the memory usage for each layer  $l_i$  increases by  $\mathcal{O}(l_{i+1}n^2 + l_in)$  when using Sherman-Morrison and  $\mathcal{O}(l_{i+1} * l_i^2)$  using the straightforward inverse for weights  $W^{(i)}$  of the size  $l_i \times l_{i+1}$ .

Besides the number of samples  $S$ , the minibatch size  $b$  and learning rate  $\eta$ , two other hyperparameters have been introduced: the damping factor  $\alpha$  needed to invert the estimation of the FIM computed from the samples when it is not full rank, and the number of steps  $K$  during which the FIM is frozen, i.e., it is not updated with respect to the new minibatch, for computational efficiency. Hyperparameter tuning for the learning rate  $\eta$ , the damping factor  $\alpha$  and the value for  $K$  are presented in the Appendix A.

Our experiments show that appropriate values for  $\alpha$  are in the range 0.01 to 0.2, depending on the network topology. The larger the conditioning number of the FIM of the largest layer, which can be formulated also as, the bigger the difference between  $n$  and  $\max(l_i)$ , the larger  $\alpha$  should be chosen. We also found that  $K$  can be kept relatively high with values of 100 and 1,000 with almost no loss in performance, but with a significant gain in time.

This result shows that during training it is possible to avoid to continuously re-estimate the geometry of the manifold of probability distributions, through the computation of the estimation of the FIM at each iteration, and that instead a local approximation is sufficient to speed-up the convergence using the natural gradient. A plausible explanation for this behavior is given by the use of the Tikhonov regularization which allows to obtain more robust estimations for the FIM.

Our final update rules are:

$$\begin{aligned}\theta_{t+1} &= \theta_t - \eta \tilde{F}_p^{-1} \nabla L_p(\theta_t) \\ \phi_{t+1} &= \phi_t - \frac{\eta}{2} \tilde{F}_q^{-1} (\nabla L_q(\phi_t) + \nabla L_{qW}(\phi_t)) .\end{aligned}\tag{33}$$

Where  $L_p$ ,  $L_q$  and  $L_{qW}$  are empirical loss functions for the wake, sleep and q-wake phases respectively. These values are computed with minibatches of size  $b$  and sampled  $S$  times. The empirical FIMs  $\tilde{F}_p^{-1}$  and  $\tilde{F}_q^{-1}$  are also estimated with  $b$  and  $S$  based on the formulas (28),(29) and (32). The pseudo-code for NRWS is presented in Alg. 1.

## 7 Natural Bidirectional Helmholtz Machine

As discussed in the introduction, the actual state of the art method for training HMs is the Bidirectional Helmholtz Machine (BiHM) [11], which optimises the log likelihood of the probability distribution

$$p^*(x) = \left( \frac{1}{Z} \sqrt{p(x, h)q(x, h)} \right)^2 ,\tag{34}$$

where  $Z$  is the normalization constant. The big advantage of this method is that both  $p$  and  $q$  distributions are learned simultaneously without the need for alternating phases, however the update rules for these distributions in practice are the same as the **wake** and **q-wake** phases only with different weights  $\tilde{\omega}_k$ .

If we want to calculate the FIM of this distribution  $p^*$  we very quickly run into the problem that it does not factorize nicely to any block-diagonal structure but to a fully dense matrix. We know already that a dense FIM would be impractical to use in any capacity for the Natural Gradient.

We could use the same FIMs  $\tilde{F}_p$  and  $\tilde{F}_q$  for the weights  $W$  and  $V$  as in the NRWS case, however these do not have a relation to the FIM of  $p^*$ , that we know of, they are not an estimations of  $p^*$  block-diagonal elements. We call this model the Natural Bidirectional Helmholtz Machine (NBiHM) and we present in section 9.3 how this construction behaves in practice.

## 8 Convergence Analysis

The convergence of the wake-sleep algorithm has been studied by Ikeda et al. [41]. In this work the authors show conditions for the theoretical convergence of a modified version of the Wake-Sleep algorithm, identified as a variant of the geometric *em* algorithm. The convergence of the *em* and their relation to the Expectation Maximization (EM) optimization process is known in literature and in particular has been studied by Fujiwara et al. [42] and Amari [43].

Ikeda et al. [41] study the convergence of Wake-Sleep first on the factor analysis model. They point out that the wake-phase is a gradient flow of the m-step. If the algorithm then “sleeps well” by sleeping for multiple steps until convergence, this is equivalent to the e-step in the *em* algorithm and thus the procedure converges to the MLE, being equivalent to the Generalized EM algorithm [44]. They subsequently notice how a sufficient condition for the algorithm to work on a general model is that the generative model is realizable by the recognition model, i.e.  $p_\theta(x|h) = q_\phi(x|h)$ . Typically however only one step of sleep is performed at each training iteration in the literature, which does not respect convergence guarantees but has been found to work efficiently in practice [6]. In Appendix B we compared the sleep-well algorithm with respect to the standard WS. We showed that taking multiple steps of sleep in one iteration of the algorithm allows a faster convergence, however when the convergence is measured with respect to the elapsed time, standard WS has still an advantage compared the sleep-well algorithm.

Notice that the algorithm by Ikeda et al. is using the exact FIM, while in the present work we are employing an estimation of the gradients and of the FIM. RWS and NRWS are using multiple samples for training the model and for estimation of the FIM, they thus do not compromise the convergence properties of WS, limited only by the quality of the statistical estimations. Further studies on the convergence properties of RWS and NRWS in relation to the number of samples used for training represents an interesting research direction and will be object of future work.

## 9 Experiments

For the final performance evaluation of NRWS we use the binarized version of the MNIST database of handwritten digits [45] as a standardized benchmark. In addition to MNIST we show the efficacy of the NRWS on the FashionMNIST dataset and the small version of the Toronto Face Dataset (TFD). In order to test NRWS not only on binary datasets, but continuous ones as well, we resorted to a form of data augmentation, where the gray values of the images were taken as probabilities for the last layer of the HM. In the Appendix C we provide further details about how this works and we present some results on the miniMNIST dataset. The miniMNIST is a downsized binarized version of the MNIST dataset, from  $28 \times 28$  to  $14 \times 14$  (Fig. 13 in Appendix C), similar to the one used by Hinton et. al. [9]. We use the miniMNIST dataset also for brief explorational analysis of the hyperparameters shown in the Appendix A to determine good values for the learning rate, damping factor and K-step parameters.

As loss function we use in our experiments a negative log-likelihood calculated on the minibatch and samples size at each iteration since the NLL is the primary measure that is being optimised by HMs (see Eq. (5).) Preliminary analysis on the miniMNIST showed a very small standard deviation for multiple runs of the same experiment, with different seeds. We tested the miniMNIST dataset with 24 different seeds and the best hyperparameters (LR 0.002 DP 0.05 as in Table 5 and Figure 14 in the Appendix C). After 100 epochs we obtain mean log likelihood of  $-28.39$  and std 0.04 while after 200 epochs mean  $-28.20$  std 0.03. This shows that the variance is relatively small for different seeds and gets smaller over time. We repeated the multiple seed experiment on the TFD dataset as well, with the best hyperparameters, with 10 seeds and after 1000 epochs. The resulting LL on the test set was mean  $-370.0$  std 0.18. Seeing these results we can safely conclude that the algorithm is robust against randomness and that there is no growing variance problem (usually associated to the REINFORCE algorithm and its variants). Based on these observations we only present one run per experiment with the confidence that they behave as an average run.

In all the experiments we worked with an epoch budget and a time budget for the NRWS, or until the algorithm converged. For the Figures 3 and 4 we used an epoch budget of 2,000 and a time budget of 70,000 seconds which corresponds to roughly 20 hours. To compensate for these long running times we ran the RWS till up to 2,500 epochs, in order for the curves to be comparable in wall-clock time as well with a reasonable certainty.

In addition to RWS we compared NRWS also to a version of it where we only use the diagonal components of the FIM, which we noted DNRWS in the experiments. DNRWS is a rougher approximation of the FIM but it is much faster to invert so we are assessing whether it is a good trade-off. We give some details about the calculation and performance of the DNRWS in the Appendix E. We always present the best parameters (learning rate,  $K$  and  $\alpha$ ) for each experiment per training algorithm, optimized for the 2,000 epochs for the plot comparisons.

All experiments were run with CUDA optimized Tensorflow 1.15 [46] on



Nvidia GTX1080 Ti GPUs. Our implementation is publicly available at <https://github.com/szokejokepu/natural-rws>.

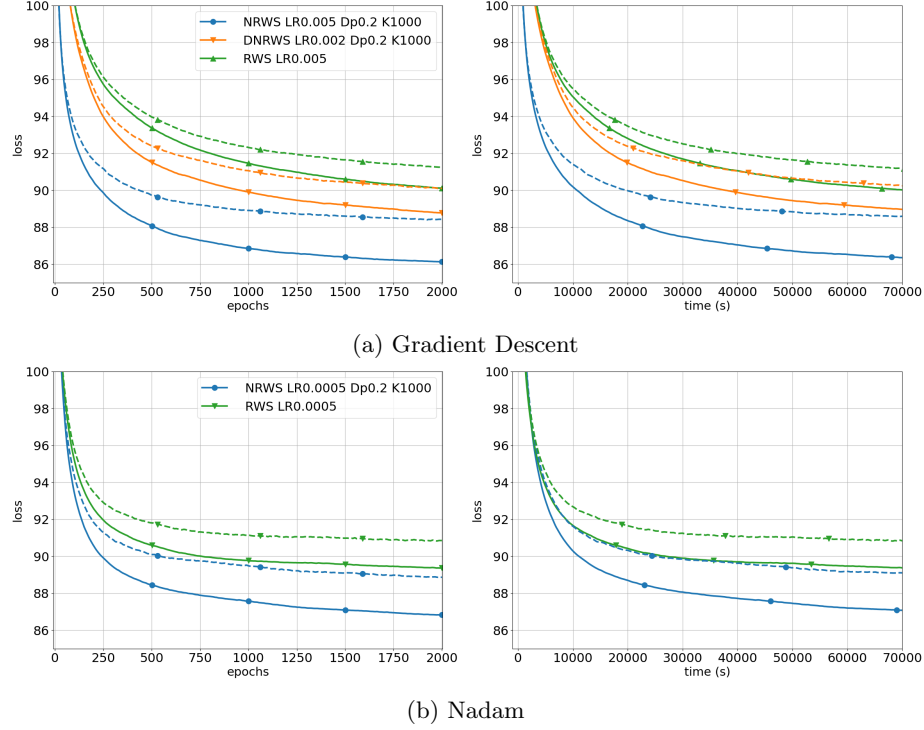


Figure 3: Training curves for MNIST for (a) Gradient Descent and (b) Nesterov Adaptive Momentum (Nadam), continuous lines represent the quantities on the train set, and dashed lines the ones on validation. Left: Loss of algorithms in epochs; Right: Loss of algorithms in wall-clock time (s) [LR=learning rate, Dp=Damping factor  $\alpha$ , K=K-step]

## 9.1 MNIST

We use the model architecture of a binary Helmholtz Machine with layers of sizes 300, 200, 100, 75, 50, 35, 30, 25, 20, 15, 10, 10, used also by Bornschein et al. [11]. The training is performed without data augmentation, with binary variables in  $\{-1, 1\}$ . We used a minibatch size of 32 for all experiments and no regularizers or decaying learning-rate for any of the algorithms.

In Fig. 3a and Table 1 we report results of experiments on the MNIST dataset with hyperparameters for each individual algorithm, based on the preliminary hyperparameter tuning. The experiments are performed with a binarized dataset, equivalently to other benchmarks in literature [10, 11]. In Fig. 3a we present loss curves during training, for training and validation. The advantage of the

NRWS in this case comes in the form of convergence to a better minimum. NRWS converges faster than the their non-geometric counterparts in epochs. Even increasing the learning rate of RWS it is not possible to achieve the same convergence speed (left panel of Fig. 3a). In time (right panel), NRWS is faster than vanilla RWS, even if the time for each epoch is roughly 25% worse. Furthermore NRWS is able to reach a better optimum at convergence.

alg	S	lr	$\alpha$	K	LL	T/E
WS	10	0.002	-	-	-90.56	30s
RWS	10	0.002	-	-	-87.36	34s
DNRWS	10	0.002	0.2	-	-86.88	39s
NRWS	10	0.002	0.2	1000	<b>-84.91</b>	43s
VAE [4]	-	-	-	-	$\approx$ -89.5	-
RWS [10]	10-100	0.001-0.0003	-	-	$\approx$ -86.0	-
BiHM [11]	10-100	0.001-0.0003	-	-	$\approx$ -85.0	-

Table 1: Importance Sampling estimation of the log-likelihood (**LL**) on the test set with 10,000 samples for different algorithms after training till convergence with SGD. **T/E** is the average time per epoch, **S** is the number of samples in training,  $\alpha$  is damping factor and **K** from K-step. The values for VAE, RWS and BiHM (Bidirectional Helmholtz Machine) are reported from [11] however the **T/E** are not comparable because of different hardware used in the experiments.

The natural gradient, by pointing in the steepest direction with respect to the Fisher-Rao metric, allows for higher rates of convergence, however at the same time it might incur in premature convergence and thus reduce generalization properties. This phenomenon is known in the literature and has been already reported by other authors in different contexts [27, 25]. In our experiments we found out that tuning the damping factor was enough to regularize the experiments.

We begin by comparing our SGDs implementations of WS, RWS, DNRWS and NRWS with state-of-the-art [10, 11], see Table 1. Implementations from the literature also take advantage of accelerated gradient methods (ADAM[47]), learning-rate decay (from  $10^{-3}$  to  $3 \times 10^{-4}$ ),  $L1$  and  $L2$  regularizers and an increased number of samples towards the end of the training (from 10 to 100), in order to achieve better results. While further hyperparameter tuning could be successfully employed to improve our reported results, as well as variable learning rates, regularizers and number of samples [11], this is out of the scope of the present paper. Even with a simple training procedure (fixed learning rate, no regularization and fixed number of samples) we notice how the IS Likelihood on 10k samples is better than RWS as reported from the literature [10] and even slightly better than BiHM [11]. Additionally, when training till convergence, the difference between the DNRWS and NRWS becomes more significant, it is obvious the rough approximation of the DNRWS is missing information that would be needed for a better final result.

Additionally, we tested the algorithms using the Nadam (Nesterov-Adam)

optimizer [48, 49, 47]. In Fig. 3b we see that the NRWS also benefits from the accelerated gradient method outperforming in epochs as well as in real-world time the RWS. We observe that while the RWS does seem to be more comparable than in the SGD case, it is still not enough to beat the NRWS either in epochs or in seconds.

The adaptive steps and the accumulated momentum of Nadam are implicitly assuming an Euclidean metric in the tangent space, which is clearly not the geometrically correct approach. This motivates the exploration of adaptive Riemannian gradient methods for the NRWS algorithm, as a future work. The IS Likelihood estimations (in Appendix D) are comparable with SGD in Table 1.

## 9.2 Toronto Face Dataset and FashionMNIST

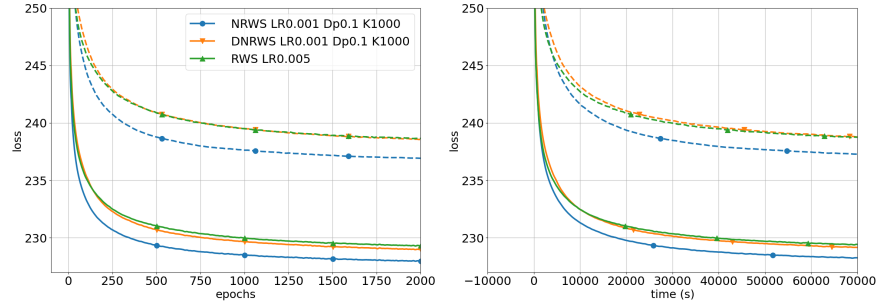
We tested NRWS on a resized version of the Toronto Face Dataset (TFD) [50] and on the Fashion MNIST dataset [51]. We used a  $24 \times 24$  resized version for the TFD to be able to use only dense layers. Given the absence in the literature of experiments on HM with RWS on those datasets, we performed comparisons with our implementation of RWS and NRWS. Our implementation of RWS has been showed to perform as well as the one in the literature, see Table 1.

We used a similar setting for experiments for each of the datasets, as for the MNIST. The same sample and minibatch size and architecture was used for the RWS and NRWS, but the learning rate and damping factor was individually tuned for each algorithm. For FashionMNIST we used the same network as for the MNIST experiments and for TFD we used 300, 200, 100, 75, 50, 35, 30, 25, 20, 20, which is very similar, but wider at the last layer.

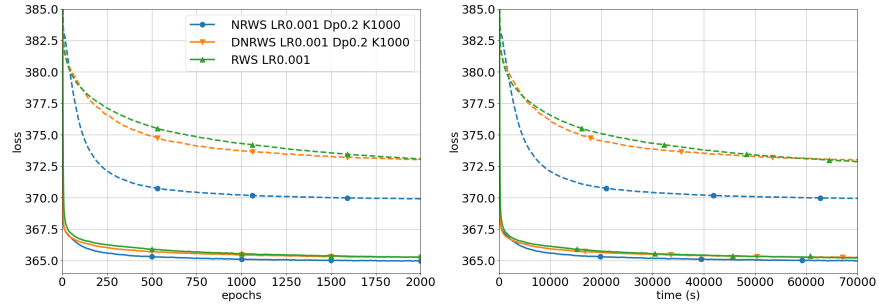
DS	alg	s	lr	$\alpha$	K	LL	T/E
FashionMNIST	RWS	10	0.004	-	-	-236.96	38s
	NRWS	10	0.002	0.1	1000	<b>-235.65</b>	51s
TFD	RWS	10	0.002	-	-	-372.73	30s
	NRWS	10	0.002	0.2	1000	<b>-370.05</b>	39s

Table 2: Importance Sampling estimation of the log-likelihood (**LL**) on the test set with 10,000 samples for different algorithms after training till convergence with SGD. **T/E** is the average time per epoch, **s** is the number of samples in training,  $\alpha$  is damping factor and **K** is from K-step. The values for RWS are from our own implementation.

In the results in the Figures 4 we can observe similar curves to what we saw in the case of the MNIST. Even the best learning rate for the RWS it can't catch up with the NRWS neither in epochs, nor in real-world time on both datasets. In the case of the TFD in particular we see a pretty big difference in the algorithms' ability to generalize. The test curve of the NRWS performs much better than the RWS. In Table 2 we see similar results as for MNIST. The NRWS outperforms RWS on both datasets on the test set. In the case of the DNRWS the issues with using a rougher estimation of the FIM becomes very apparent,



(a) NRWS with gradient descent for FashionMNIST



(b) NRWS with gradient descent for TFD



(c) Generated FashionMNIST images



(d) Generated TFD images

Figure 4: Training curves for FashionMNIST (a) and TFD (b) with Gradient Descent, continuous lines represent the quantities on the train set, and dashed lines the ones on validation; Left: Loss of algorithms in epochs; Right: Loss of algorithms in wall-clock time (s) (c) and (d) Example images generated with NRWS after 2000 epochs for the FashionMNIST and TFD. [LR=learning rate, Dp=Damping factor  $\alpha$ , K=K-step]

as for both datasets the method underperformed even to the RWS. Clearly, for more complex image datasets, such as FashionMNIST and TFD, the structure of the FIM of the model cannot be restricted any more than the block-structure

described in Proposition 1, as it leads to sub-optimal performance.

### 9.3 Bidirectional Helmholtz Machine on MNIST

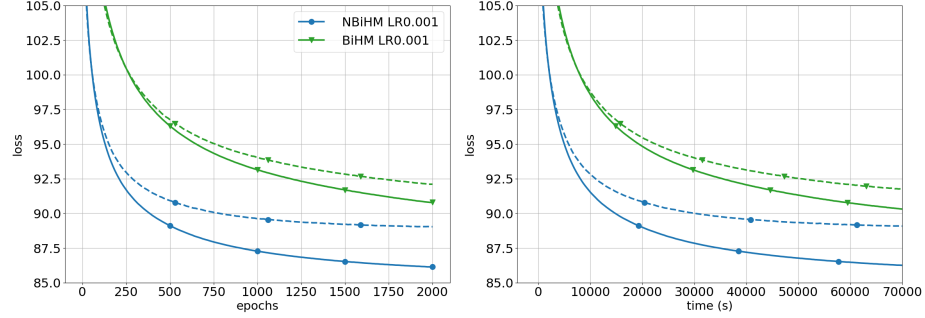


Figure 5: Training curves for MNIST for the BiHM and NBiHM algorithms, continuous lines represent the quantities on the train set, and dashed lines the ones on validation. Left: Loss of algorithms in epochs; Right: Loss of algorithms in wall-clock time (s) [LR=learning rate, Dp=Damping factor  $\alpha$ , K=K-step]

We repeated a simplified version of the experiment on MNIST with the BiHM presented in the original paper [11] and we compare it to our NBiHM implementation. Similarly to our previous experiments we performed them without gradient acceleration, regularization and adaptive sample size.

As a result we notice in Figure 5 that applying the natural gradient does benefit the BiHM in convergence rate and final convergence minimum even though it is not the right FIM being used. These results are somewhat confounding as we know it is not the right geometry being used, which would be using a FIM associated to the  $p^*$  from (34). The same finding is mirrored in the Table 3. A further observation from the table is that the big advantage of the NBiHM versus the NRWS is its running time. Since the NBiHM is doing two update rules which are equivalent to the Wake and an Wake-q updates up to different reweighting factors, while the NRWS has a total of 3 phases, the NBiHM takes significantly less time for an epoch compared to the NRWS. However we could not reach the same accuracy with NBiHM as with the NRWS, which could be the side-effect of not using the right FIM.

## 10 Conclusions

We showed how the graphical structure of Helmholtz Machines allows the efficient computation of the Fisher information matrix and thus the natural gradient during training, by exploiting the locality of the connection matrix. The resulting structure of the FIM is a smaller grained block-diagonal matrix than what is generally used in the literature which leads to a more efficient

alg	s	lr	$\alpha$	K	LL $p$	LL $p^*$	T/E
BiHM	10	0.001	-	-	-87.6	-90.745	29
NBiHM	10	0.001	0.1	1000	<b>-86.18</b>	<b>-89.21</b>	38s
NRWS	10	0.002	0.2	1000	<b>-84.91</b>	-	43s

Table 3: Importance Sampling estimation of the log-likelihood (**LL**) for both  $p$  and  $p^*$  on the test set for MNIST with 10,000 samples for different algorithms after training till convergence with SGD. **T/E** is the average time per epoch, **s** is the number of samples in training,  $\alpha$  is damping factor and **K** is from K-step. The values for BiHM and NBiHM are from our own implementation.

estimation. In such models it is not required to introduce any extra conditional independence assumption between random variables for computing the natural gradient efficiently, due to the sparse structure of the Fisher information matrix and the presence of explicit analytical formulas for the computations of its blocks. We introduced the Natural Reweighted Wake-Sleep (NRWS) algorithm and we demonstrated an improvement of the convergence during training for stochastic gradient descent. NRWS was not only faster to converge, but the obtained optimum resulted in better values for the IS likelihood estimation compared to the values obtained with RWS [10] and BiHM [11] on MNIST. These findings have been corroborated by additional experiments on continuous datasets as FashionMNIST and Toronto Face Dataset. Again, on both of these datasets, the NRWS outperformed the vanilla RWS version in both convergence speed and quality of the converged optimum, while also exhibiting a better generalization gap.

The  $K$ -step update version of the Natural Reweighted Wake-Sleep algorithm showed considerable speed-up in terms of training time, without a decrease in performance. Noticeably, we showed how a rough and delayed estimation of the Fisher information matrix, in the context of our experiments, was enough to achieve state-of-the-art performances for HM. The damping factor introduced in training effectively acts as a regularizer reducing the gap between train and validation. Studying the effects of geometrical regularization over the weights, time dependent damping factor,  $K$  step or learning rate, in order to further boost performances will be object of future studies.

As detailed in Section 5 the complexity of the algorithm is dominated by  $\mathcal{O}(l_0(l_1n + n^{2.32}))$  where  $l_0$  and  $l_1$  are the bottom two layers of the Helmholtz Machine, which are usually the largest, and  $n = b * S$  is minibatch size per sample size, and there is also an increased memory usage. Hence, the current version of the algorithm does not scale well for larger datasets with higher resolution and color images from the literature, for which the computational time will grow with the complexity formula above, in particular since  $l_0$  and  $l_1$  will grow. Future investigations will aim to speed up the NRWS algorithm and additionally we want to explore architectures allowing us to reduce the complexity, such as CNNs.

Moreover, we plan to further study ways to obtain a better estimation of the

FIM. Although, as we have shown in the case of the DNRWS, the structure of the FIM cannot be further simplified, additional techniques to refine and accumulate the FIM estimation over time could be beneficial for the training. When using the Nadam optimizer, NRWS seems to maintain the speed advantage and the convergence to a better optimum, compared with its non-geometric counterpart. This encourages the exploration of adaptive gradient methods for the Natural Reweighted Wake-Sleep in which the Fisher-Rao metric is explicitly considered for the momentum accumulation and the adaptive step.

As a final remark, we highlight that since the computation of the Fisher information matrix is only dependent on the underlying statistical model, other algorithms for the training of HMs could benefit from the use of the natural gradient, such as Bidirectional Helmholtz Machine [11].

## 11 Acknowledgements

Váradý, Volpi and Malagò have been partially supported by the DeepRiemann project, co-funded by the European Regional Development Fund and the Romanian Government through the Competitiveness Operational Program 2014-2020, Action 1.1.4, project ID P\_37\_714, contract no. 136/27.09.2016.

## References

- [1] G. E. Hinton, S. Osindero, Y.-W. Teh, A fast learning algorithm for deep belief nets, *Neural computation* 18 (7) (2006) 1527–1554.
- [2] Y. Bengio, Learning Deep Architectures for AI, *Foundations and Trends® in Machine Learning* 2 (1) (2009) 1–127. doi:10.1561/22000000006.
- [3] I. Goodfellow, Y. Bengio, A. Courville, *Deep learning*, MIT press, 2016.
- [4] D. P. Kingma, M. Welling, Auto-encoding variational bayes, *International Conference on Learning Representations - ICLR*, arXiv:1312.6114 (2014).
- [5] D. J. Rezende, S. Mohamed, D. Wierstra, Stochastic backpropagation and approximate inference in deep generative models, in: E. P. Xing, T. Jebara (Eds.), *Proceedings of the 31st International Conference on Machine Learning*, Vol. 32 of *Proceedings of Machine Learning Research*, PMLR, Beijing, China, 2014, pp. 1278–1286.
- [6] P. Dayan, G. E. Hinton, R. M. Neal, R. S. Zemel, The Helmholtz Machine, *Neural computation* 7 (5) (1995) 889–904.
- [7] R. M. Neal, Connectionist learning of belief networks, *Artificial intelligence* 56 (1) (1992) 71–113.
- [8] X. Glorot, Y. Bengio, Understanding the difficulty of training deep feed-forward neural networks, in: *Proceedings of the thirteenth international conference on artificial intelligence and statistics*, 2010, pp. 249–256.

- [9] G. E. Hinton, P. Dayan, B. J. Frey, R. M. Neal, The "wake-sleep" algorithm for unsupervised neural networks, *Science* 268 (5214) (1995) 1158–1161.
- [10] J. Bornschein, Y. Bengio, Reweighted Wake-Sleep, International Conference on Learning Representations, arXiv:1406.2751 [cs]ArXiv: 1406.2751 (2015).
- [11] J. Bornschein, S. Shabanian, A. Fischer, Y. Bengio, Bidirectional Helmholtz Machines, in: International Conference on Machine Learning, PMLR, 2016, pp. 2511–2519.
- [12] L. Wenliang, T. Moskovitz, H. Kanagawa, M. Sahani, Amortised learning by wake-sleep, in: International Conference on Machine Learning, PMLR, 2020, pp. 10236–10247.
- [13] L. Hewitt, T. Anh Le, J. Tenenbaum, Learning to learn generative programs with Memoised Wake-Sleep, in: J. Peters, D. Sontag (Eds.), Proceedings of the 36th Conference on Uncertainty in Artificial Intelligence (UAI), Vol. 124 of Proceedings of Machine Learning Research, PMLR, 2020, pp. 1278–1287.
- [14] S. L. Lauritzen, Graphical Models, Oxford University Press, 1996.
- [15] R. J. Williams, Simple statistical gradient-following algorithms for connectionist reinforcement learning, *Machine learning* 8 (3-4) (1992) 229–256.
- [16] A. Mnih, K. Gregor, Neural variational inference and learning in belief networks, in: International Conference on Machine Learning, PMLR, 2014, pp. 1791–1799.
- [17] G. Tucker, A. Mnih, C. J. Maddison, D. Lawson, J. Sohl-Dickstein, Rebar: Low-variance, unbiased gradient estimates for discrete latent variable models, in: 31st Conference on Neural Information Processing Systems, 2017.
- [18] W. Grathwohl, D. Choi, Y. Wu, G. Roeder, D. Duvenaud, Backpropagation through the void: Optimizing control variates for black-box gradient estimation, in: International Conference on Learning Representations, 2018.
- [19] W. Kool, H. van Hoof, M. Welling, Estimating gradients for discrete random variables by sampling without replacement, in: International Conference on Learning Representations, 2020.
- [20] S.-I. Amari, Natural gradient works efficiently in learning, *Neural computation* 10 (2) (1998) 251–276.
- [21] S.-i. Amari, Neural learning in structured parameter spaces-natural Riemannian gradient, in: Advances in neural information processing systems, 1997, pp. 127–133.
- [22] S.-i. Amari, H. Nagaoka, Methods of information geometry, Vol. 191, American Mathematical Soc., 2000.



- [23] G. Desjardins, R. Pascanu, A. Courville, Y. Bengio, Metric-free natural gradient for joint-training of boltzmann machines, International Conference on Learning Representations; (2013).
- [24] G. Desjardins, K. Simonyan, R. Pascanu, et al., Natural neural networks, in: Advances in Neural Information Processing Systems, 2015, pp. 2071–2079.
- [25] R. Grosse, J. Martens, A kronecker-factored approximate fisher matrix for convolution layers, in: International Conference on Machine Learning, 2016, pp. 573–582.
- [26] Y. Ollivier, Riemannian metrics for neural networks I: feedforward networks, Information and Inference: A Journal of the IMA 4 (2) (2015) 108–153.
- [27] J. Martens, R. Grosse, Optimizing neural networks with kronecker-factored approximate curvature, in: International conference on machine learning, 2015, pp. 2408–2417.
- [28] K. Sun, F. Nielsen, Relative fisher information and natural gradient for learning large modular models, in: Proceedings of the 34th International Conference on Machine Learning-Volume 70, JMLR. org, 2017, pp. 3289–3298.
- [29] W. Lin, M. E. Khan, N. Hubacher, D. Nielsen, Natural-gradient stochastic variational inference for non-conjugate structured variational autoencoder, International Conference on Machine Learning (2017).
- [30] G. Zhang, S. Sun, D. Duvenaud, R. Grosse, Noisy natural gradient as variational inference, in: J. Dy, A. Krause (Eds.), Proceedings of the 35th International Conference on Machine Learning, Vol. 80 of Proceedings of Machine Learning Research, PMLR, 2018, pp. 5852–5861.
- [31] N. Ay, Locality of global stochastic interaction in directed acyclic networks, Neural Computation 14 (12) (2002) 2959–2980.
- [32] A. Graves, Practical variational inference for neural networks, in: Advances in neural information processing systems, 2011, pp. 2348–2356.
- [33] T. A. Le, A. R. Kosiorek, N. Siddharth, Y. W. Teh, F. Wood, Revisiting Reweighted Wake-Sleep for models with stochastic control flow, in: Uncertainty in Artificial Intelligence, PMLR, 2020, pp. 1039–1049.
- [34] S.-i. Amari, Differential-geometrical methods in statistics, Lecture Notes on Statistics 28 (1985) 1.
- [35] S.-i. Amari, Information geometry and its applications, Vol. 194, Springer, 2016.
- [36] N. Ay, J. Jost, H. Vân Lê, L. Schwachhöfer, Information geometry, Vol. 64, Springer, 2017.

- [37] H. Park, S.-I. Amari, K. Fukumizu, Adaptive natural gradient learning algorithms for various stochastic models, *Neural Networks* 13 (7) (2000) 755 – 764.
- [38] N. Ay, On the locality of the natural gradient for learning in deep Bayesian networks, *Information Geometry* (Nov 2020). doi:10.1007/s41884-020-00038-y.
- [39] Y. Ollivier, L. Arnold, A. Auger, N. Hansen, Information-geometric optimization algorithms: A unifying picture via invariance principles, *Journal of Machine Learning Research* 18 (18) (2017) 1–65.
- [40] S.-i. Amari, H. Park, K. Fukumizu, Adaptive method of realizing natural gradient learning for multilayer perceptrons, *Neural computation* 12 (6) (2000) 1399–1409.
- [41] S. Ikeda, S.-i. Amari, H. Nakahara, Convergence of the Wake-Sleep Algorithm, in: *Advances in neural information processing systems*, 1999, pp. 239–245.
- [42] A. Fujiwara, S.-i. Amari, Gradient systems in view of information geometry, *Physica D: Nonlinear Phenomena* 80 (3) (1995) 317–327.
- [43] S.-I. Amari, Information geometry of the EM and em algorithms for neural networks, *Neural networks* 8 (9) (1995) 1379–1408.
- [44] G. J. McLachlan, T. Krishnan, *The EM algorithm and extensions*, Vol. 382, John Wiley & Sons, 2007.
- [45] Y. [dataset] LeCun, C. Cortes, C. Burges, *Mnist handwritten digit database* (2010).
- [46] M. Abadi, A. Agarwal, P. Barham, E. Brevdo, Z. Chen, C. Citro, G. S. Corrado, A. Davis, J. Dean, M. Devin, S. Ghemawat, I. Goodfellow, A. Harp, G. Irving, M. Isard, Y. Jia, R. Jozefowicz, L. Kaiser, M. Kudlur, J. Levenberg, D. Mané, R. Monga, S. Moore, D. Murray, C. Olah, M. Schuster, J. Shlens, B. Steiner, I. Sutskever, K. Talwar, P. Tucker, V. Vanhoucke, V. Vasudevan, F. Viégas, O. Vinyals, P. Warden, M. Wattenberg, M. Wicke, Y. Yu, X. Zheng, *TensorFlow: Large-scale machine learning on heterogeneous systems*, software available from tensorflow.org (2015). URL <https://www.tensorflow.org/>
- [47] D. P. Kingma, J. Ba, Adam: A method for stochastic optimization, *International Conference on Learning Representations - ICLR*; arXiv:1412.6980 (2015).
- [48] N. S. Keskar, R. Socher, Improving generalization performance by switching from ADAM to SGD, *arXiv preprint arXiv:1712.07628* (2017).

- [49] A. C. Wilson, R. Roelofs, M. Stern, N. Srebro, B. Recht, The marginal value of adaptive gradient methods in machine learning, in: *Advances in Neural Information Processing Systems*, 2017, pp. 4148–4158.
- [50] J. M. [dataset] Susskind, A. K. Anderson, G. E. Hinton, The Toronto Face Database, Department of Computer Science, University of Toronto, Toronto, ON, Canada, Tech. Rep 3 (2010).
- [51] H. [dataset] Xiao, K. Rasul, R. Vollgraf, Fashion-mnist: a novel image dataset for benchmarking machine learning algorithms, *arXiv preprint arXiv:1708.07747* (2017).
- [52] K. G. Kirby, A tutorial on Helmholtz Machines, Department of Computer Science, Northern Kentucky University (2006).

# Appendix

## A Hyperparameter tuning

In this section we will present more in details some preliminary experiments and hyperparameters tuning principles. In addition to the datasets used in the paper we used the miniMNIST dataset and the ThreeByThree (denoted in the following as 3by3) synthetic dataset. The 3by3 dataset was introduced by Kirby [52] which consists of a 3by3 grid with vertical and horizontal patterns, represented in Fig. 9a (left). The advantage of this dataset is that the true  $KL$  divergence value between the *generation distribution*  $p$  and the *true distribution* of the data  $p^*$  can be calculated very precisely, and we don't have to rely solely on the approximation of the log-likelihood by importance sampling which is traditionally used to evaluate generative models. The 3by3 converges very quickly to a minimum, so the rate of convergence can be monitored in steps rather than epochs. These datasets were mainly used as preliminary results to explore the ranges of the hyperparameters quickly and serve as preliminary comparisons between WS, RWS and NRWS.

### A.1 Learning Rate and Damping Factor

Ideally we want to find the smallest damping factor which still maintains the optimization stable. Too large damping factors lead to an optimization similar to the non natural algorithms, while too small damping factors lead to a large conditioning number in the estimated FIM, whose inversion then carries serious numerical issues. This behaviour can be seen clearly in Fig. 6. We searched empirically for the right combination of learning rate and damping factor leading to the best convergence rate.

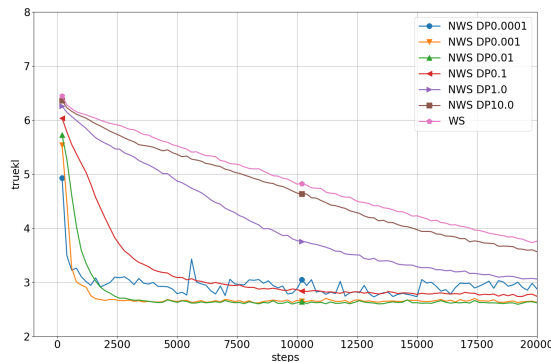


Figure 6: The loss with different damping values for the 3by3 dataset.

For the 3by3 dataset we determined a range of 0.001 – 0.1 for damping values that outperform the vanilla algorithm (Fig. 6). As one can observe, with very

low damping the algorithm converges almost instantly but the loss remains noisy, as each small modification in the FIM is amplified when applied to the gradient. Large values however lead to convergence that is similar to the one of WS. From this general range the parameter has to be fine-tuned for each dataset/model, to determine the appropriate combination of learning rate versus damping factor.

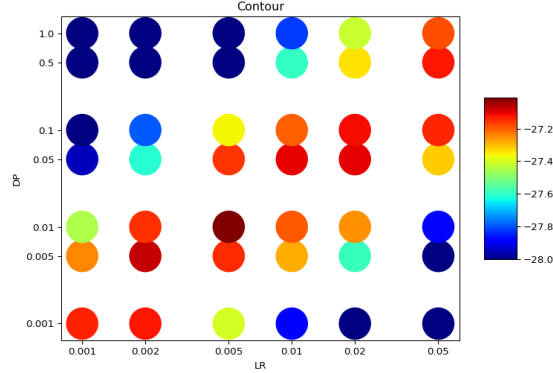


Figure 7: The minimum loss of experiments in relation to Learning rate and Damping factor, on a model with 100, 50, 20, 10, 10 layers.

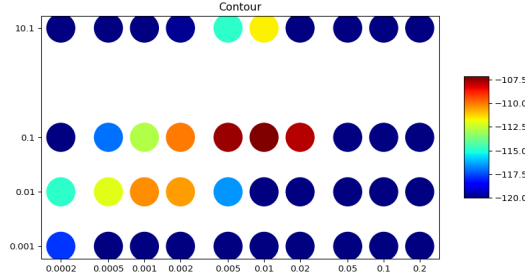


Figure 8: The minimum loss of experiments in relation to Learning rate and Damping factor, on a model with 200,100,10 layers.

In Fig. 7 and Fig. 8 we compare different learning rates and damping factors on a smaller architecture to determine the appropriate quantities for optimal convergence in the case of the miniMNIST and MNIST. We determine that the appropriate damping factor for this dataset with similar models is around 0.005 – 0.1, with a learning rate in the neighbourhood of 0.005 – 0.02.

We can notice the expected linear relation between learning rate and damping factor. When we grow the damping factor, we can also grow the learning rate up to a given point. The explanation for this phenomenon is that (as shown in

Section 5 Inversion of the FIM, in the main paper) the smaller the damping, the closer the algorithm is to following the geometry of the manifold defined by the statistical model. Thus smaller steps lead to better improvements, also a larger damping mitigates instabilities due to few-samples statistical estimations.

We also observe a correlation between the size of the image and the magnitude of the damping factor. The larger the image in the first layer, the more samples are needed to estimate the FIM of the network accurately. When the number of samples cannot be grown anymore for practical reasons (the complexity of the algorithm grows quadratically with the number of samples), a larger damping factor is needed so the matrix can have a reasonable conditioning number.

## A.2 K-step

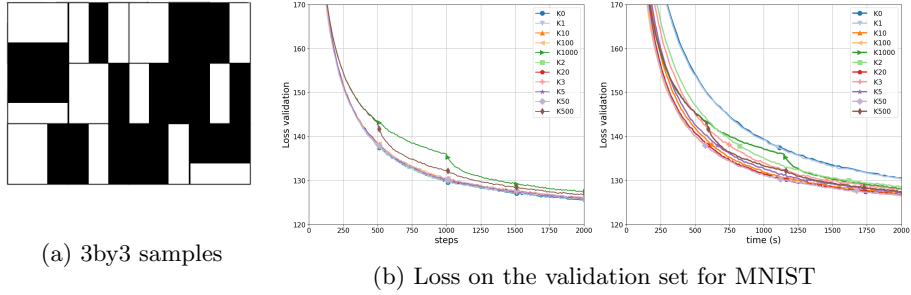
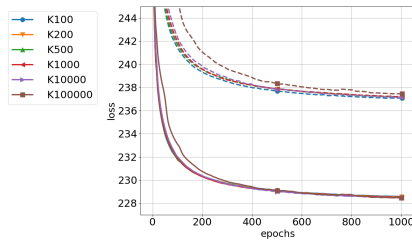


Figure 9: (a) Samples from the 3by3 dataset; (b) Loss curves for MNIST for different values of  $K=\{0,1,2,3,5,10,20,50,100,500,1000\}$ ; left: in epochs; right: in seconds

Once found the best combination of hyperparameters for the Natural Wake-Sleep optimizer, we explore the possibility to compute the FIM only every  $K$ -steps and thus speed up the computational time of the algorithm. In Fig. 9b we see the changes in the loss on the validation set for MNIST for a fixed learning rate and damping factor. We observe that for a  $K$ -steps the algorithm speeds up significantly, but loses stability at very high values, which is most noticeable in the case of  $K = 1000$  steps, and to a lesser degree for  $K = 500$ . Consequently we can use a  $K$ -step in the range of  $[1, 100]$  without noticeable impact on the performance of the algorithm. In our experiments we used  $K = 50$  or  $K = 100$ .

However, the analysis we did thus far on  $K$ -step was mainly focused on the short term effects. To thoroughly explore the effects of the  $K$ -step, we analyze the convergence of the NRWS on the FashionMNIST dataset, we fix learning rate 0.001 and damping factor 0.1 while varying  $K$ . In Figure 10 we can see that clearly  $K = 100000$  is pushing the algorithm too far, as it breaks down on both the train and test curves. All-in-all we notice that most of the curves converge to the same minimum, contrary to what we might have expected from the previous experiment. However there is a significant difference in the time an epoch takes in Table 4. Furthermore we can notice a slight advantage in the test curve for



K	median. time (s)
100	286.17
200	234.74
500	207.63
1,000	201.74
10,000	191.10
100,000	184.28

Figure 10: Loss curves for train and test on FashionMNIST for different values of  $K$

Table 4: Average time per epoch for different values of  $K$

$K = 100$ , which hints at keeping the  $K$  value as low as possible might still bring some advantage. We conclude that  $K$  values in the range of 100 – 1000 are the most preferable, which are acceptable from a speed and final convergence perspective. This result seem quite surprising and might hint to the fact that for some problems the metric on the manifold is varying slowly from point to point.

## B Sleep-well

As preliminary exploratory analysis we studied briefly the Sleep-well variant of Wake-Sleep. As mentioned in Section 8 WS only has theoretical convergence guarantees for the variant where the sleep phase is done until convergence after every wake phase. At the best of our knowledge there are no studies in the literature using this variant. It is usually commonly accepted to use WS as a simple alternating algorithm, with one step of each phase instead.

In Figure 11 we compare 4 variants of the WS on miniMNIST, with the same hyperparameters as above, where we only changed the number of sleep steps: 1, 3, 5, 10 per one wake step. We see that there is a noticeable difference between the variants, with more sleep steps resulting in better convergence in epochs. Looking at the real-time comparisons of the experiments, the conclusion takes a different perspective. The time penalty for the multiple sleep phases ends up slowing down the algorithm significantly, with an amount that scales linearly with the number of steps.

Further in Figure 12 we studied how the sleep-well affects the NRWS and also its long term affects. We noticed that the NRWS also benefits from extra steps in the sleep cycle, however seemingly to a less degree than the WS. We also tested rescaling the learning rate in the sleep phase, because taking a larger step could benefit the algorithm in a similar way as taking more but smaller steps. We found that slightly increasing the length of the sleep step with a factor of 3 does benefit both WS and NRWS. The benefit of increasing the size rather than the number of steps is that it does not come with any extra time penalty, however taking more steps achieves consistently better minimums. Doing both larger and more steps, however negatively impacts the algorithm (see red line in

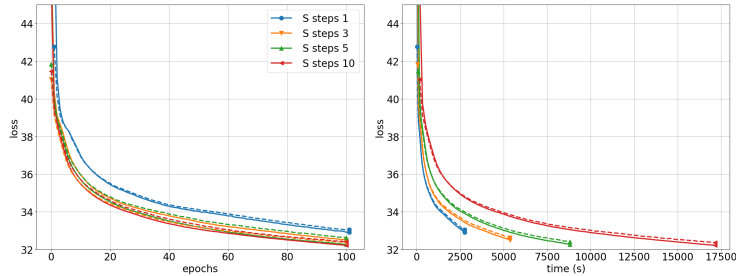


Figure 11: Loss on the train and validation sets of the miniMNIST with different 1, 3, 5, 10 sleep steps for every wake step

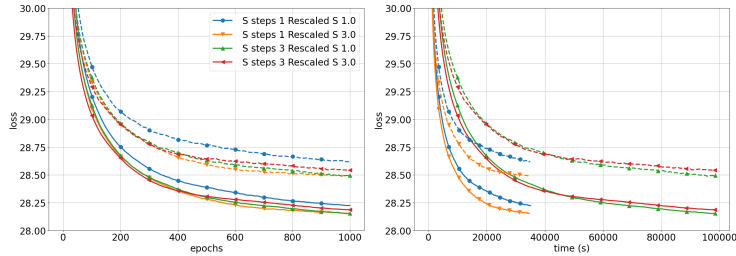


Figure 12: Loss on the train and validation sets of the miniMNIST with different 1, 3 sleep steps and 1 or 3 times rescaled sleep steps for NRWS

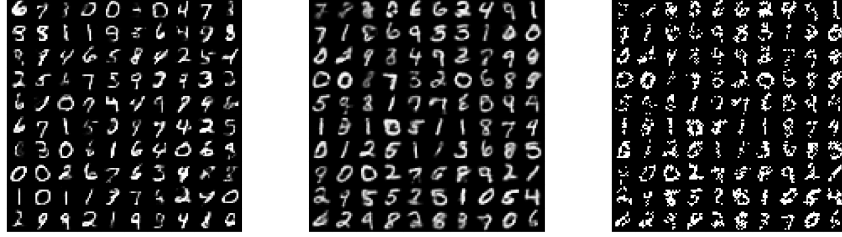
Figure 12).

Given the relatively small loss improvement of Figures 11 and 12, we decided to opt for the original solution with 1 sleep step and with the same size as the wake phase. This solution is the fastest time-wise and it is inline with all other works from the literature, that we compare to, thus we used the standard single sleep step through all of our experiments.

## C Data augmentation

We compare two different strategies to learn a binary dataset. The first approach is to simply binarize all the samples from the dataset once, by rounding to  $\{0, 1\}$ , which we call **B**. This technique is used for benchmarking usually and on average have smaller log likelihoods. The second technique, Binary Stochastic or Continuous **C**, is to take the gray values as the means to a Bernoulli distribution, for each sample from the dataset and for each pixel in the image. This form of data augmentation is enabling us to use continuous data, it is also used commonly in the literature [11]. At each training step we sample from the distributions, thus we get a range of samples, from a single image, which together approximate the original continuous example better than **B**. In Fig 13 (a) and (b) we see samples from models thought with the differing techniques where we see that





(a) miniMNIST B. probs (b) miniMNIST C. probs (c) miniMNIST samples

Figure 13: miniMNIST Dataset examples

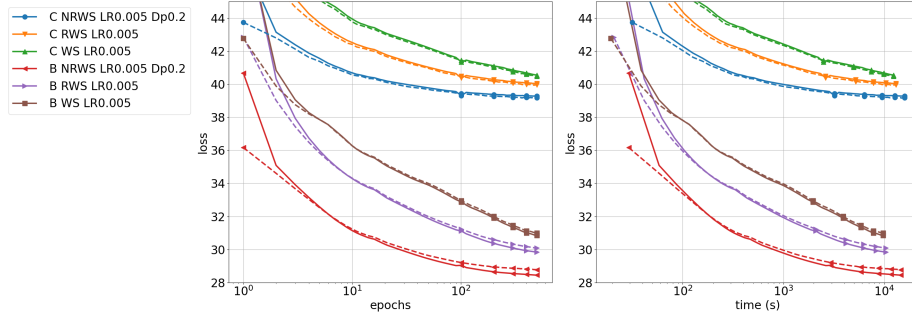


Figure 14: The loss of training miniMNIST until convergence with **B** and **C**, with the algorithms WS, RWS and NRWS with the layers of the size 100,50,20,10,10. On the left the convergence in epochs and on the right convergence in wall-clock time (s), both in log-scale [LR=learning rate, Dp=Damping factor  $\alpha$ ].

the **C** creates clearly more realistic images. We use the same technique for TFD in the main paper in Figure 4d

In Fig 14 we compare the loss curves for three different models WS, RWS and NRWS and the two strategies and in Table 5 for the miniMNIST dataset, we report the importance sampled approximation of the log-likelihood. We can see that in all cases the NRWS eventually outperforms both models both in achieving the better minimum, as well as in the rate of convergence and wall-clock time. Moreover, a clear advantage is visible early on in the training, in the case of the **B** from the 15<sup>th</sup> epoch and in **C** from the very beginning.

## D Results for NRWS with Nadam

As we can see in Table 6 also when we use Nesterov-Adam (Nadam) instead of SGD (as in the main paper), the NRWS converges to a better minimum, but worse than simple SGD (reported in Table in the main paper).

DS	alg	lr	LL	T/E
<b>B</b>	WS	0.04	-29.337	19s
	RWS	0.02	-28.695	21s
	NRWS	0.004	<b>-27.606</b>	31s
<b>C</b>	WS	0.02	-38.232	23s
	RWS	0.01	-37.811	25s
	NRWS	0.004	<b>-36.578</b>	32s

Table 5: Importance Sampling estimation of the log-likelihood (**LL**) with 10,000 samples for different algorithms after 500 epochs of training with SGD. **T/E** is the average time per epoch. The damping factor used for NRWS is 0.05. For all algorithms, the number of samples used in training is 10.

alg	s	lr	LL	T/E
RWS	10	0.0002	-86.987	34s
NRWS	10	0.001	<b>-85.675</b>	44s

Table 6: Importance Sampling estimation of the log-likelihood (**LL**) with 10,000 samples for different algorithms after training till convergence with Nadam. The damping factor used is 0.1. **T/E** - average time per epoch; **s** - samples in training.

## E Diagonal Natural Reweighted Wake-Sleep

The Diagonal Natural Reweighted Wake-Sleep (DNRWS) is a version of the NRWS where we approximate the FIM by taking only its diagonal elements. In the case of the HM it is easy to calculate, instead of performing the calculations in (26) and (28) we can just calculate

$$F_{p,j}^{(i)} = \frac{1}{n} \sum \sigma' \left( W_j^{(i)} h^{(i+1)} \right) (h^{(i+1)})^2 \quad \text{and} \quad (35)$$

$$F_{q,j}^{(i)} = \frac{1}{n} \sum \sigma' \left( V_j^{(i)} h^{(i-1)} \right) (h^{(i-1)})^2. \quad (36)$$

Inverting the matrices becomes trivial since the FIM is diagonal, calculating the reciprocal is computationally very easy. In fact because it is much faster, we can calculate the FIM approximation in every gradient step, with no need to save it for  $K$  steps.

Analyzing how the change in the hyperparameters of the learning rate and damping factor  $\alpha$  in Figure 15 it reveals that the best combination is similar to the one used for NRWS. Taking a smaller  $\alpha$  leads to quicker convergence, but worse minimum, with some instability when closer to convergence. Larger damping leads to a more stable convergence, but a slower one, compensating by speeding up with a larger learning rate leads to premature convergence.

In Figure 16 we compare the DNRWS to NRWS and RWS for a shorter period of 500 epochs, a full comparison till convergence can be seen in Figure

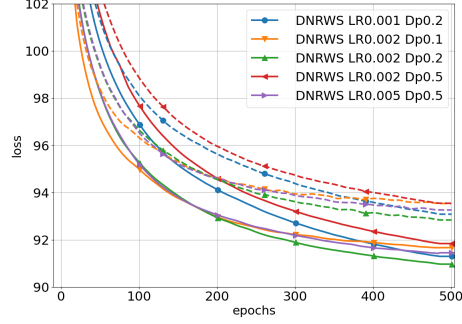


Figure 15: Loss of training (continuous line) and validation (dashed line) on MNIST with different Learning Rates and Damping Factors for the DNRWS [LR=learning rate, Dp=Damping factor  $\alpha$ ]

3a in the main paper. We see a speedup of the DNRWS compared to the RWS, but the achieved minimum is worse than that of the NRWS. This observation is inline with what we were expecting as the diagonal approximation of the FIM leads to worse results than the estimation of the actual structure. In wall-clock time the DNRWS is a bit more promising, as it manages to outperform both RWS and NRWS for a longer period, which could be viewed as benefit in some cases. All other hyperparameters like sample and minibatch-size was kept the same for all algorithms.

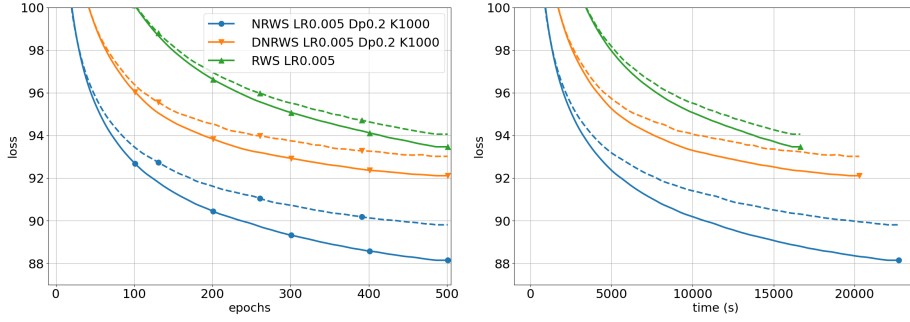


Figure 16: Loss of training (continuous line) and validation (dashed line) of RWS, DNRWS and NRWS on MNIST; (right) epochs (left) seconds of 500 epochs [LR=learning rate, Dp=Damping factor  $\alpha$ , K=K-step]